 CMES, vol.89, no.6, pp.459-480, 2012

# Fatigue Crack Growth Study and Remaining Life Assessment of High Strength and Ultra High Strength Concrete Beams

**A. Ramachandra Murthy[1], Nagesh R. Iyer[1] and B.K. Raghu Prasad[2]**

**Abstract:** This paper presents the details of crack growth study and remaining life assessment of concrete specimens made up of high strength concrete (HSC, HSC1) and ultra high strength concrete (UHSC). Flexural fatigue tests have been conducted on HSC, HSC1 and UHSC beams under constant amplitude loading with a stress ratio of 0.2. It is observed from the studies that (i) the failure patterns of HSC1 and UHSC beams indicate their ductility as the member was intact till the crack propagated up to 90% of the beam depth and (ii) the remaining life decreases with increase of notch depth (iii) the failure of the specimen is influenced by the frequency of loading. A "Net K" model has been proposed by using non-linear fracture mechanics principles for crack growth analysis and remaining life prediction. SIF (K) has been computed by using the principle of superposition. SIF due to the cohesive forces applied on the effective crack face inside the process zone has been obtained through Green's function approach by applying bi-linear tension softening relationship to consider the cohesive the stresses acting ahead of the crack tip. Remaining life values have been have been predicted and compared with the corresponding experimental values and observed that they are in good agreement with each other.

**Keywords:** Ultra high strength concrete; characterization; fatigue loading; Tension softening, Stress intensity factor; crack growth; remaining life

## 1 Introduction

Concrete has been one of the most commonly used construction materials in the world. One of the major problems civil engineers face today is concerned with preservation, maintenance and retrofitting of structures. The historical develop-

[1] CSIR-Structural Engineering Research Centre, Taramani, Chennai, India, 600113, [murthyarc, nriyer] @serc.res.in

[2] Civil Engineering Dept., Indian Institute of Science, Bangalore, bkr@civil.iisc.ernet.in

ment of concrete material may be marked and divided into several stages. The first is the traditional normal strength concrete (NSC), where only four kinds of ingredients, namely, cement, water, fine aggregates and coarse aggregates are used. With the increasing development in physical infrastructure, such as high-rise buildings, long-span bridges, flyovers, power plant structures, higher compressive strength concrete is preferred in most cases. When the compressive strength of concrete is generally higher than 50 MPa, it is usually defined as high strength concrete (HSC). The easiest way to reach high compressive strength is to reduce the water–cement ratio. Therefore, in HSC, the fifth ingredient, the water reducing agent or superplasticizer, is found to be indispensable. However, sometimes the compressive strength is not as important and necessary as some other properties, such as low penetrability, high durability and excellent workability. Thus, high performance concrete (HPC) was proposed and widely studied at the end of the last century [Peiwei et al. 2001] . An ultra high strength concrete (UHSC) with axial compressive strength of more than 100 MPa and also with a high tensile strength (more than 10% of the compressive strength) has been successfully developed [Richard and Cheyrezy 1994,1995; Mingzhe et al. 2010; Goltermann et al. 1997].

According to classical theory, applied load result in in-plane tensile stresses at the bottom of the structures/component. The stress state in such structures is often simulated with three point bending tests and modulus of rupture calculations. Concrete beams subjected to flexural loading fails owing to crack propagation. Repeated loading results in a steady decrease in the stiffness of the structure, eventually leading to failure. It is of interest to characterize the material behaviour subjected to such loading and study the crack propagation resulting from such loading. Fibers are added to overcome the limited tensile capacity of concrete. The fibers alter the mechanical characteristics of the material, especially after the matrix has cracked by bridging across the cracks and providing some post-cracking ductility and fracture toughness. The bridging reduces the stress intensity at the crack tip and higher energy is required for crack extension. The amount of additional energy required for crack extension depends mainly on the physical and material properties of the fibers and the matrix. For many structures, the live load varies in a repetitive manner, for example forces developed by wind, trains, vehicular traffic, often inducing vibrations. The design of such structures requires knowledge of the behavior of the building materials under repetitive loading [Bazant 1992; Bazant and Pfeiffer 1987).

The governing mechanisms in fatigue of concrete are not yet completely understood. In general, there are two hypotheses regarding crack initiation and its evolution. The first hypothesis is that the mechanism of fatigue failure, which is attributed to progressive deterioration of the bond between the coarse aggregate and

the matrix. This phenomenon seems more or less to be intensified, if the modulus of elasticity of the aggregate exceeds that of the material. The second hypothesis is that fatigue failure in concrete occurs because of the growth of pre-existing microcracks in the material. With increasing deformation, the microcracks coalesce, resulting in a single macro-crack. The development of this process weakness the section up to the point, where it can no longer maintain the applied load. The evolution of cracking in concrete structures requires rational modeling to obtain more reliable predictions of structural response to earthquake, traffic loads, environmental change and various other severe loads. Repeated loading causes crack to grow. This phenomenon, called fatigue fracture, was studied extensively for metals and ceramics. For concrete, however, the knowledge of fatigue fracture is limited. A few experimental investigations on fatigue crack propagation in concrete were reported by kaplan [1961], Bazant et al. [1991;1993], Ingraffea [1977], Baluch et al. [1987]. The rate of fatigue crack growth in concrete exhibits an acceleration stage that follows an initial deceleration stage. In the deceleration stage the rate of crack growth decreases with increasing crack length, whereas in the acceleration stage, there is a steady increase in crack growth rate up to failure. Fracture mechanics principles were applied to describe the crack growth during the acceleration stage of fatigue crack growth in concrete. It was observed that the Paris law coefficients are dependent on the material composition potentially explaining the large differences in the values of the Paris law coefficients. These investigations indicated that the application of the Paris law for crack growth due to repeated loading can be used from metals to concrete with appropriate modifications. These studied were carried out by Kaplan [1961], Baluch et al. [1987], Bazant et al. [1991;1993], Perdikaris et al. [1987], Subramaniam et al. [2000], Matsumoto and Li [1999], Toumi and Turatsinze [1998]. Mingzhe et al. [2010] evaluated fatigue life of reactive powder concrete specimens by conducting experiments under single and multi- level amplitude. Little analytical work has been carried out on crack growth of concrete [Prasad and Krishnamoorthy 2002; Gasser and Holzapfel 2005; Wu et al. 2006; Slowik et al. 2006].This paper presents the details of crack growth study and remaining life assessment of concrete specimens made up of high strength concrete (HSC, HSC1) and ultra high strength concrete (UHSC) under constant amplitude load.

## 2 Properties of materials

The materials used for the development of HSC, HSC1 and UHSC and their corresponding mechanical properties are discussed below. For HSC, the ingredient materials are Portland cement, coarse aggregate, fine aggregate and water, whereas for HSC1, the materials are Portland cement, silica fume, quartz sand, high range

water reducer, water and steel fibers. Further, for UHSC, the materials are Portland cement, silica fume, quartz sand, quartz powder, high range water reducer, water and steel fibers. The main difference between HSC or HSC1 and UHSC is the addition of quartz powder in the case of HSC1 mix. The materials used for the development of high strength concrete (HSC, HSC1) and ultra high strength concrete (UHSC) are shown in Table 1. Properties of the materials used to make HSC, HSC1 and UHSC are given below.

**Cement**

- Grade - 53 (OPC)
- Particle size range - 31 $\mu$m to 7.5 $\mu$m
- Compressive strength:

28 – Days strength - 57 MPa

**Silica fume (SF)**

- Particle size range - 0.2 to 25$\mu$m

**Quartz powder (QP)**

- Particle size range - 2.3 $\mu$m to 75 $\mu$m

**Quartz sand**

- Particle size range - 400 $\mu$m to 800 $\mu$m

**Steel fibers**

- Length - 13 mm
- Diameter - 0.18mm
- Yield stress - 1500 MPa

**Standard sand**

- Particle size range - 0.5mm to 0.09mm (Grade 3 of IS:650 )

**Coarse aggregate**

- Particle size range - 4.75mm to 20 mm

**Super plasticizers (SP)**

Polycarboxylate ether based superplasticizer is used. Appearance - Light yellow coloured liquid.

The specimen preparation process was strictly controlled to minimize scatter in the test results. In case of HSC, the sample preparation is as usual and curing was done in routine way, but for HSC1 and UHSC specimens, immediately after demoulding, the specimens were fully immersed in potable water at room temperature for 2 days. After 2 days, the specimens were placed in a autoclave at 90˚C for 2 days. The specimens were placed in oven at 200˚C for 1 day followed by autoclave curing. Compressive tests were carried out on cylindrical specimens of 150×300 mm (diameter×height) in the case of HSC and 75x150mm in the case of HSC1 and UHSC. Table 2 shows the mechanical properties of concrete.

Table 1: Mix ratio of HSC, HSC1 and UHSC

| Mix | Cement | Fine aggregate | Coarse aggregate | Silica fume | Quartz sand | Quartz powder | Steel fiber | Water | SP % |
|---|---|---|---|---|---|---|---|---|---|
| HSC | 1 | 1.25 | 2.48 | - | - | - | - | 0.45 | - |
| HSC1 | 1 | - | - | 0.25 | 1.5 | - | 2% | 0.33 | 2.5 |
| UHSC | 1 | - | - | 0.25 | 1.1 | 0.4 | 2% | 0.23 | 3.5 |

From Table 2, it can be observed that the split tensile strength for the case of HSC is 4.0 MPa. It is about 7% of compressive strength. In the case of HSC1, the split tensile strength is about 18% of compressive strength. The increase in strength is significant compared to HSC. The increase in strength may be due to various sizes of ingredients and steel fibres. Further, it can be observed from Table 2 that UHSC has high compressive strength and tensile strength. The high strengths can be attributed to the contribution at different scales viz., at the meso scale due to the fibers and at the micro scale due to the close packing of grains which is on account of good grading of the particles.

Table 2: Mechanical properties of HSC, HSC1 and UHSC

| S. No | Mix ID | Compressive Strength (MPa) | Split tensile Strength (MPa) | Modulus of elasticity (MPa) |
|---|---|---|---|---|
| 1. | HSC | 57.14 | 3.96 | 35,780 |
| 2. | HSC1 | 87.71 | 15.38 | 37,890 |
| 3. | UHSC | 122.52 | 20.65 | 42,987 |

## 3 Casting and testing of beams

The specimens of various sizes have been cast for HSC, HSC1 and UHSC. The quality of the concrete is maintained as uniform as possible. Three identical specimens for each notch depth and size of the beam have been cast. The beam moulds have been filled with concrete in three layers and each layer is compacted well using a table vibrator. Notches of various depths have been cut in beam specimens using a cutting machine. The ratios of notch/ beam depth are 0.1, 0.2, 0.3 and 0.4. The notch width is around 3 mm. The pictorial view of notched beam specimens is shown in Figure 1. The ratio of span to depth is considered as 4.0. Details of the specimens prepared for experimental study and notch depth details are given in Tables 3, 4 and 5. The experimental setup consists of a MTS 2500 kN capacity servo hydraulic UTM with online data acquisition system. Appropriate load cells have been used for testing. Figure. 2 shows a typical experimental setup. A series of HSC, HSC1 and UHSC beams have been tested under central point flexural fatigue loading.

Figure 1: Typical Notched Beam Specimens

A stress ratio of 0.2 is maintained for all the specimens. Frequency of loading is varied for the specimens. At regular intervals, crack depth vs number of cycles has been recorded for HSC1 and UHSC specimens. Tables 3 to 5 show the maximum load ($P_{max}$) , minimum load ($P_{min}$), frequency of loading and no. of cycles to failure. $P_{max}$ has been arrived at based on the failure load obtained from the static test. It can be observed from Tables 3 to 5 that the remaining life increases with the increase of beam depth and decreases with increase of notch depth. Further, it can be observed that the no of cycles are influenced by the frequency of loading and type of specimen. The pictorial representation of the failure pattern of HSC, HSC1


Figure 2: Typical Experimental Setup

and UHSC beams under fatigue loading are shown in Figure 3. Paris crack growth constants have been evaluated from the experimental data of $da/dN$ and $\Delta K$. The values of C and m for various cases are shown in Table 7.

It is clear from these studies that the fibers are able to provide sufficient tensile reinforcement across the cracks and have sufficient fatigue resistance to stabilize the response of the specimen under these loading conditions. Additionally, some multiple cracks have been noticed around the crack tip, for some specimens. Such crack branching would increase the energy demand for further crack propagation, thereby increasing local fracture toughness. The multiple crack formation may be due to the presence of flaws near the crack tip. The failure patterns of HSC1 and UHSC beams indicate ductility as of the member was intact till the crack propagated up to 90% of the beam depth. This type of study will be useful for design of similar type of specimens/structures subjected to fatigue loading.

## 4 Net K model considering tension softening

In the Net K model, non-linear fracture mechanics principles have been used for crack growth analysis and remaining life prediction. The merits of the model are two fold; (i) it is possible to get SIF variation from crack initiation to unstable crack propagation (ii) it is possible to model the fatigue behavior. SIF (K) has been computed by using the principle of superposition. More importantly, the method of superposition employed in the net K model follows from the method adopted by Dugdale, Irwin while doing plasticity correction in metals. Infact, the material UHSC is closer to metals and such a method would be more appropriate. The mechanism under fatigue loading in HSC1 & UHSC may be attributed to progres-

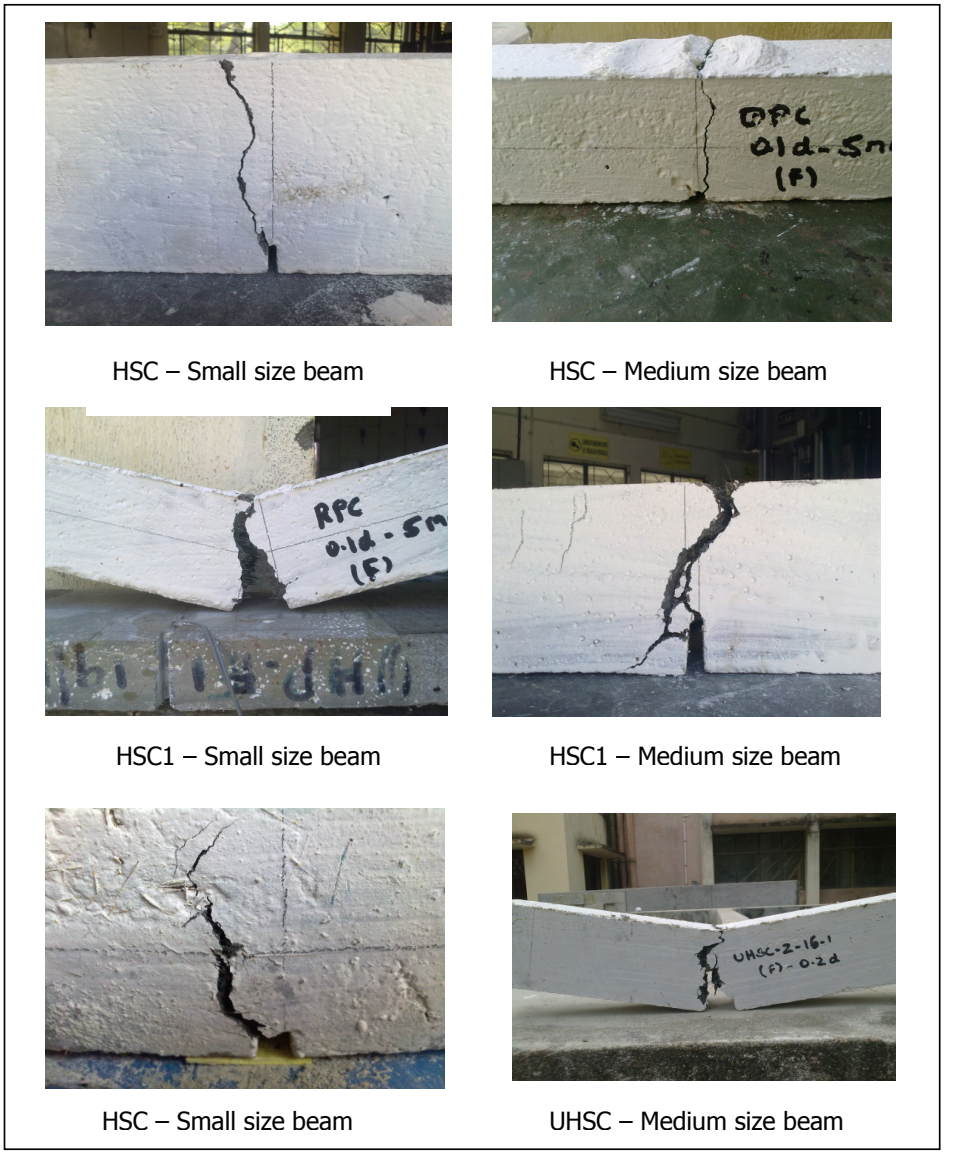


Figure 3: Failure Pattern of Beams under Fatigue Loading

Table 3: Remaining Life Evaluation of HSC Specimens

| S. No | Dimension (mm) | Notch depth (mm) | $P_{max}$ (kN) | $P_{min}$ (kN) | Frequency of loading (Hz) | No. of Cycles to failure |
|---|---|---|---|---|---|---|
| 1. | 250 x 50 x 50 | 0.1 d | 1.90 | 0.38 | 0.3 | 2219 |
| 2. | | 0.1 d | | | | 2423 |
| 3. | | 0.2 d | 1.39 | 0.277 | | 1623 |
| 4. | | 0.2 d | | | | 1516 |
| 5. | | 0.3 d | .715 | 0.143 | | 1094 |
| 6. | | 0.3 d | | | | 1120 |
| 7. | 500 x 50 x 100 | 0.1 d | 2.71 | 0.54 | 0.3 | 5412 |
| 8. | | 0.1 d | | | | 5729 |
| 9. | | 0.2 d | 1.803 | 0.361 | | 4316 |
| 10. | | 0.2 d | | | | 4118 |
| 11. | | 0.3 d | 1.323 | 0.264 | | 2916 |
| 12. | | 0.3 d | | | | 3012 |
| 13. | 1000 x 50 x 200 | 0.1 d | 5.09 | 1.018 | 0.3 | 7816 |
| 14. | | 0.1 d | | | | 8102 |
| 15. | | 0.2 d | 4.39 | 0.88 | | 6412 |
| 16. | | 0.2 d | | | | 6019 |
| 17. | | 0.3 d | 3.177 | 0.64 | | 5312 |
| 18. | | 0.3 d | | | | 5069 |

sive bond deterioration between aggregates and matrix or by development of cracks existing in the concrete matrix. These two mechanisms may act together or separately, leading to complexity of the fatigue mechanism. It is well known fact that concrete typically exhibits nonlinear fracture processes because of the large FPZ, leading to LEFM based approach becoming objectionable. Hence, an analytical model for assessing the fatigue life of concrete accounting the tension softening effect is required. The following are the basic assumptions of tension softening.

Modelling assumptions

1. Plane sections of the beam remain plane after deformation
2. Fictitious crack surface remains plane after deformation
3. Normal closing tractions acting on the fictitious crack follow the linear stress crack opening displacement
4. Bending stress in the concrete along the bottom of the beam is equal to the traction normal to the crack mouth at the bottom of the beam.

Table 4: Remaining Life Evaluation of HSC1 specimens

| S. No | Dimension (mm) | Notch depth (mm) | $P_{max}$ (kN) | $P_{min}$ (kN) | Frequency of loading (Hz) | No. of Cycles to failure |
|---|---|---|---|---|---|---|
| 1. | 250 x 50 x 50 | 0.1 d | 3.36 | 0.673 | 0.5 | 2012 |
| 2. | | 0.1 d | | | | 1914 |
| 3. | | 0.2 d | 2.69 | 0.54 | | 1621 |
| 4. | | 0.2 d | | | | 1592 |
| 5. | | 0.3 d | 2.27 | 0.45 | | 1031 |
| 6. | | 0.3 d | | | | 1124 |
| 7. | | 0.4 d | 1.682 | 0.34 | | 824 |
| 8. | | 0.4 d | | | | 886 |
| 9. | 500 x 50 x 100 | 0.1 d | 6.67 | 1.335 | 0.5 | 3219 |
| 10. | | 0.1 d | | | | 2946 |
| 11. | | 0.2 d | 4.081 | 0.816 | | 2714 |
| 12. | | 0.2 d | | | | 2678 |
| 13. | | 0.3 d | 3.193 | 0.64 | | 2120 |
| 14. | | 0.3 d | | | | 1980 |
| 15. | | 0.4 d | 2.55 | 0.51 | | 1401 |
| 16. | | 0.4 d | | | | 1512 |

To incorporate the tension softening behaviour, based on the principle of superposition, SIF has to be modified as (Figure 4),

$$K_I = K_I^P + K_I^q \tag{1}$$

where $K_I$ is called net K and $K_I^q$ is negative

where $K_I^P$ is SIF for the concentrated load P on a 3 point bend specimen, and $K_I^q$ is SIF due to the closing force applied on the effective crack face inside the process zone, which can be obtained through Green's function approach by knowing the appropriate softening relation

SIF due to the concentrated load P can be calculated by using LEFM principles. A three-point bending beam is shown in Figure 4. The SIF for the beam can be expressed as

$$K_I^p = \sigma\sqrt{\pi a}\, g_1\left(\frac{a}{b}\right) \text{ where, } \sigma = \frac{3PS}{2b^2t} \tag{2}$$

where P= applied load, a= crack length, b= depth of the beam, t= thickness and $g_1$(a/b)= geometry factor, depends on the ratio of span to depth of the beam and is

Table 5: Remaining Life Evaluation of UHSC Specimens

| S. No | Dimension (mm) | Notch depth (mm) | $P_{max}$ (kN) | $P_{min}$ (kN) | Frequency of loading (Hz) | No of Cycles to failure |
|---|---|---|---|---|---|---|
| 1. | 250 x 50 x 50 | 0.1 d | 8.0 | 1.6 | 0.5 | 2062 |
| 2. | | 0.1 d | | | | 2112 |
| 3. | | 0.2 d | 6.5 | 1.3 | | 1354 |
| 4. | | 0.2 d | | | | 1464 |
| 5. | | 0.3 d | 4.9 | 0.9 | | 1172 |
| 6. | | 0.3 d | | | | 1015 |
| 7. | | 0.4 d | 3.3 | 0.7 | | 820 |
| 8. | | 0.4 d | | | | 764 |
| 9. | 400 x 50 x 80 | 0.1 d | 11.3 | 2.3 | 0.5 | 5416 |
| 10 | | 0.1 d | | | | 5621 |
| 11. | | 0.2 d | 8 | 1.6 | | 3922 |
| 12. | | 0.2 d | | | | 4152 |
| 13. | | 0.3 d | 6.1 | 1.2 | | 3102 |
| 14. | | 0.3 d | | | | 3215 |
| 15. | | 0.4 d | 4.4 | 0.8 | | 2432 |
| 16. | | 0.4 d | | | | 2319 |
| 17. | 650 x 50 x 130 | 0.1 d | 17.5 | 3.5 | 0.5 | 7492 |
| 18. | | 0.1 d | | | | 7654 |
| 19. | | 0.2 d | 11.4 | 2.3 | | 4152 |
| 20. | | 0.2 d | | | | 4302 |
| 21. | | 0.3 d | 8.1 | 1.6 | | 3214 |
| 22. | | 0.3 d | | | | 3109 |
| 23. | | 0.4 d | 5.84 | 1.2. | | 2314 |
| 24. | | 0.4 d | | | | 2483 |

given below for S/b=4.0 [Tada et al. 1985]:

$$g_1\left(\frac{a}{b}\right) = \frac{1.99-(a/b)(1-a/b)[2.15-3.93a/b+2.70(a/b)^2]}{\sqrt{\pi}(1+2a/b)(1-a/b)^{3/2}} \tag{3}$$

Computation of $K_I^q$

The incremental SIF due to the closing force dq can be written as, [Shah and Swartz 1995]

$$dK_I^q = \frac{2}{\sqrt{\pi\Delta a}} dq\, g\left(\frac{a}{D}, \frac{x}{a}\right) \tag{4}$$

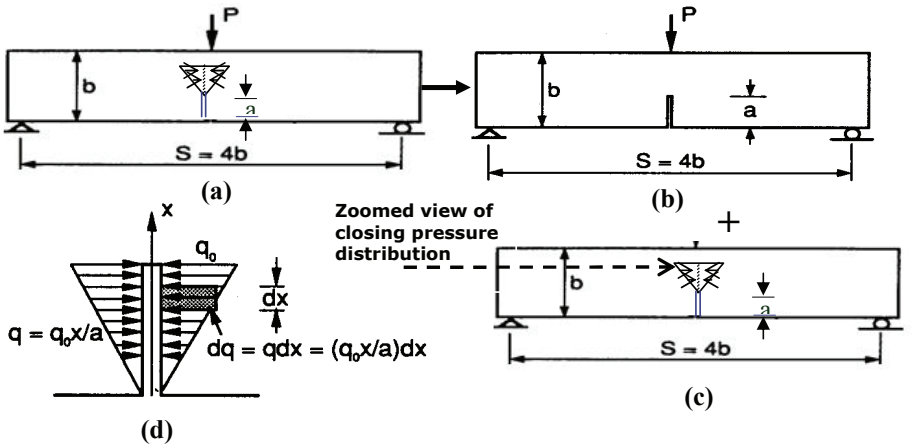


Figure 4: Illustration of superposition principle Computation of $K_I^P$

where dq can be expressed as function of softening stress distribution over the crack length Δa; the function 'g' represents the geometry factor.

Calculation of 'dq'

By using the above concept (Figure 4 (d)), cohesive crack can be modelled in the following manner (Figure 5).

The crack opening displacement w at any point x is assumed to follow linear relationship (Figure. 5) and can be expressed as,

$$w = \delta\left(\frac{a_0 - x}{\Delta a} + 1\right) \quad a_0 \leq x \leq a_{eff} \tag{5}$$

where $\delta$ is the crack opening displacement and a0 is initial crack length.

As an example, let us consider linear softening law [Shah and Swartz 1995]

$$\sigma = f_t\,(1 - w/w_c) \tag{6}$$

where, $f_t$ = tensile strength of concrete and $w_c$= critical crack opening displacement

Substituting for w from equation (5) in the linear softening law given by equation (6), one can obtain,

$$dq = \sigma = f_t\left\{1 - \frac{\delta}{w_c}\left(\frac{a_0 - x}{\Delta a} + 1\right)\right\} \tag{7}$$

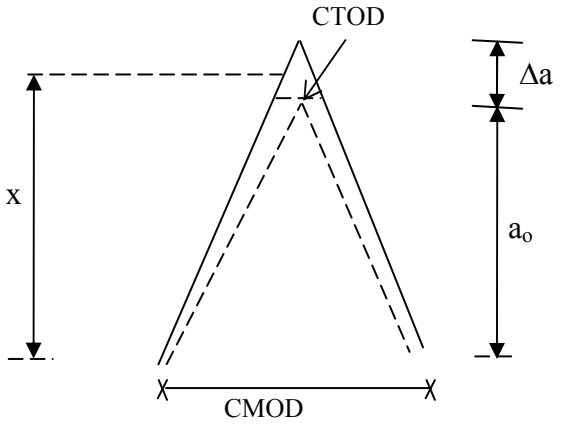


Figure 5: Cohesive crack modelling-schematic diagram of crack opening displacement

The crack opening displacement at any point $\delta(x)$ can be calculated using the following equation

$$\delta(x) = CMOD g_3\left(\frac{a}{b}, \frac{x}{a}\right) \tag{8}$$

where

$$g_3\left(\frac{a}{b}, \frac{x}{a}\right) = \left\{\left(1-\frac{x}{a}\right)^2 + \left(1.081 - 1.149\frac{a}{b}\right)\ \left[\frac{x}{a} - \left(\frac{x}{a}\right)^2\right]\right\}^{1/2}$$

where CMOD is crack mouth opening displacement and is calculated using the following formula.

$$CMOD = \frac{4\sigma a}{E} g_2\left(\frac{a}{b}\right) \tag{9}$$

where $g_2$(a/b) is geometric factor, depends on the ratio of span to depth of the beam and is given below for S = 4.0 b

$$g_2\,(a/b) = 0.76 - 2.2a/b + 3.87(a/b)^2 - 2.04(a/b)^3 + \frac{0.66}{(1-a/b)^2} \tag{10}$$

Hence, replacing dq in equation (4) and integrating over length Δa, $K_I^q$ can be obtained as,

$$K_I^q = \int_{a_0}^{a_{eff}} \frac{2f_t}{\sqrt{\pi\Delta a}}\left\{1 - \frac{\delta}{w_c}\left(\frac{a_0 - x}{\Delta a} + 1\right)\right\} g\left(\frac{a}{b}, \frac{x}{a}\right) dx \tag{11}$$

where

$$g\left(\frac{a}{b},\frac{x}{a}\right) = \frac{3.52(1-x/a)}{(1-a/b)^{3/2}} - \frac{4.35-5.28x/a}{(1-a/b)^{1/2}} + \left[\frac{1.30-0.30(x/a)^{3/2}}{\sqrt{1-(x/a)^2}} + 0.83 - 1.76\frac{x}{a}\right]\left[1-\left(1-\frac{x}{a}\right)\right]\frac{a}{b} \tag{12}$$

Similar expressions can be obtained for other models such as bilinear, trilinear, exponential, power law etc.,

### *4.1 Remaining Life Prediction*

Analysis of fatigue crack growth and remaining life prediction require data regarding loading conditions, type of material and crack geometry, among others. Then, a suitable crack growth law must be selected. One general expression for such a law is

$$\frac{da}{dN} = f(\Delta K, R, ...) \tag{13}$$

The number of loading cycles required to extend the crack from an initial length $a_0$ to the final critical crack length $a_f$ is given by

$$N = \int_{a_0}^{a_f} \frac{da}{f(\Delta K, R, ...)} \tag{14}$$

The remaining life prediction using eqn. 14 involves calculating the integral, and the procedure to be used depends, among other factors, on the type of load involved. The evaluation of this integral is much more difficult for variable amplitude loading (VAL), which introduces variability in the loading cycles and gives rise to overlapped cycles that may require the use of a counting method, namely those employing approximations based on determining growth on a cycle-by-cycle basis and those using a statistical loading definition to determine the fatigue life. The cycle-by-cycle approach involves calculating the number of cycles for each crack length increment. In general, remaining life can be predicted by using any one of the standard crack growth equations (such as Paris, Erdogan-Ratwani, etc.,). Using the Paris law,

$$\frac{da}{dN} = C(\Delta K)^m \tag{15}$$

Here, $\Delta K$ can be computed by using following expression

$\Delta K = K_{max} - K_{min}$, where $K_{max} = K^p - K^q$.

## 5 Numerical studies & discussion of results

Crack growth studies and remaining life prediction have been carried out for three point bending UHSC and HSC1 beams by using the above methodologies. Bi-linear tension softening model developed by using inverse analysis has been used to account for tension softening. Table 6 shows the tensile strength and the other parameters required for bi-linear model. Paris crack growth constants (C, m), maximum load, minimum load and predicted remaining life are shown in Table 7. Figures 3 to 7 show the plot of variation of predicted remaining life with crack depth and the corresponding experimental observations for UHSC and HSC1 beams. From Table 6 and Figures. 6 to 10, it can be observed that the predicted remaining life is in good agreement with the corresponding experimental observations. A significant advantage of net K model is that it is possible to obtain $\Delta K$ as an increment in the value of K at every step.

Table 6: Parameters of bi-linear model

| Beam dimensions (mm) | Notch depth (mm) | $f_t$ (MPa) | $w_1$ (mm) | $\sigma_1$ (MPa) | $w_2$ or $w_c$ (mm) |
|---|---|---|---|---|---|
| 250*50*50 (UHSC) | 5 | 11.6 | 0.99 | 3.6 | 3.10 |
| | 10 | 11.6 | 0.88 | 3.9 | 2.99 |
| | 15 | 11.6 | 0.89 | 3.3 | 2.99 |
| | 20 | 11.4 | 0.91 | 3.5 | 2.81 |
| 400*50*80 (UHSC) | 8 | 11.6 | 0.51 | 4.4 | 3.02 |
| | 16 | 11.4 | 0.53 | 4.3 | 2.98 |
| | 24 | 11.6 | 0.56 | 4.4 | 3.10 |
| | 32 | 11.6 | 0.54 | 4.4 | 3.00 |
| 650*50*130 (UHSC) | 13 | 11.3 | 0.41 | 4.1 | 3.01 |
| | 26 | 11.3 | 0.41 | 4.0 | 3.12 |
| | 39 | 11.5 | 0.39 | 3.9 | 3.23 |
| | 52 | 11.4 | 0.40 | 4.0 | 3.18 |
| 250*50*50 (HSC1) | 5 | 6.8 | 0.67 | 2.1 | 2.83 |
| | 10 | 6.5 | 0.59 | 2.1 | 2.79 |
| | 15 | 6.6 | 0.62 | 2.1 | 2.89 |
| | 20 | 6.6 | 0.63 | 2.1 | 2.90 |
| 500*50*100 (HSC1) | 10 | 7.0 | 0.60 | 1.9 | 2.79 |
| | 20 | 7.1 | 0.62 | 1.9 | 2.75 |
| | 30 | 7.0 | 0.61 | 2.0 | 2.80 |
| | 40 | 6.9 | 0.63 | 2.0 | 2.91 |
| | 50 | 7.1 | 0.60 | 2.0 | 2.88 |

Table 7: Remaining life predicted by net K model

| Beam dimensions (mm) | Notch depth | Max. load (kN) | Min load (kN) | Paris Crack growth constants | Remaining life, cycles | | |
|---|---|---|---|---|---|---|---|
| | | | | log C | m | Exptl | Analytical |
| 250*50*50 (UHSC) | 5 | 8.0 | 1.6 | -17.24 | 5.31 | 2112 | 1876 |
| | 10 | 6.5 | 1.3 | -16.99 | 5.23 | 1464 | 1280 |
| | 15 | 4.9 | 0.9 | -16.54 | 5.13 | 1172 | 1035 |
| | 20 | 3.3 | 0.7 | -16.35 | 5.01 | 820 | 745 |
| 400*50*80 (UHSC) | 8 | 11.3 | 2.3 | -18.78 | 6.17 | 5621 | 5223 |
| | 16 | 8 | 1.6 | -18.52 | 6.02 | 4159 | 3845 |
| | 24 | 6.1 | 1.2 | -18.23 | 5.86 | 3215 | 2876 |
| | 32 | 4.4 | 0.8 | -17.45 | 5.32 | 2432 | 2230 |
| 600*50*130 (UHSC) | 13 | 17.5 | 3.5 | -19.99 | 6.76 | 7654 | 6801 |
| | 26 | 11.4 | 2.3 | -19.34 | 6.33 | 4302 | 3910 |
| | 39 | 8.1 | 1.6 | -18.98 | 5.96 | 3214 | 2810 |
| | 52 | 5.84 | 1.2 | -18.54 | 5.69 | 2483 | 2231 |
| 250*50*50 (HSC1) | 5 | 3.36 | 0.673 | -15.46 | 5.12 | 2012 | 1812 |
| | 10 | 2.69 | 0.54 | -14.76 | 5.34 | 1617 | 1503 |
| | 15 | 2.27 | 0.45 | -15.21 | 5.01 | 1234 | 1134 |
| | 20 | 1.682 | 0.34 | -14.79 | 5.11 | 1032 | 890 |
| 500*50*100 (HSC1) | 10 | 6.67 | 1.335 | -17.23 | 6.01 | 4356 | 4089 |
| | 20 | 4.081 | 0.816 | -16.89 | 6.11 | 3219 | 2820 |
| | 30 | 3.193 | 0.64 | -16.78 | 5.99 | 2489 | 2178 |
| | 40 | 2.55 | 0.51 | -16.56 | 5.67 | 1876 | 1694 |

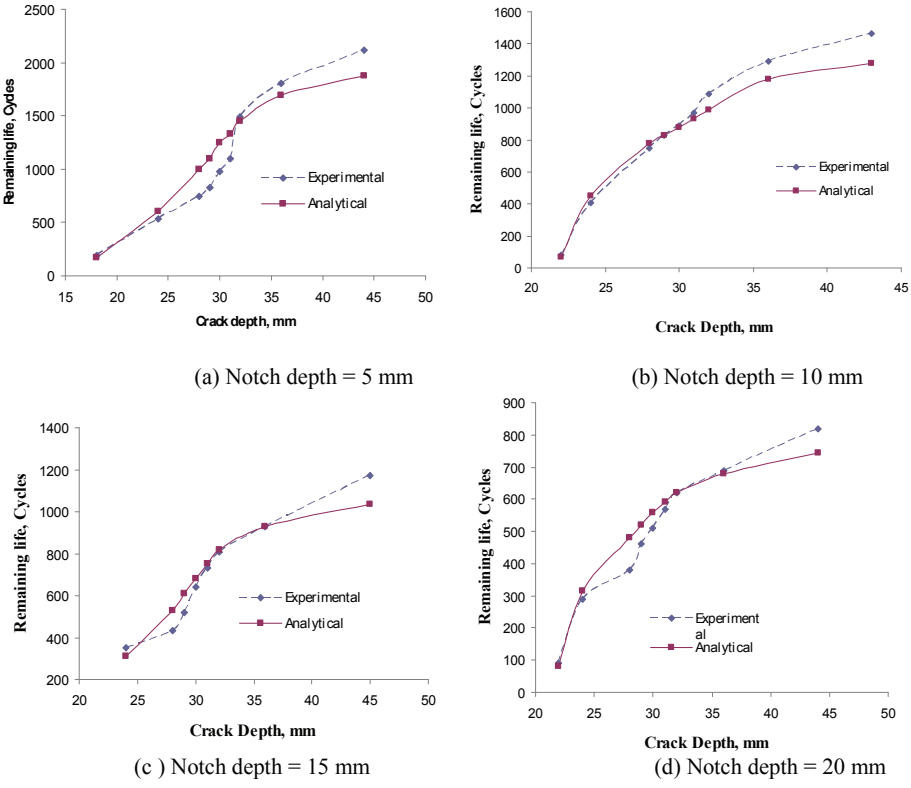


(a) Notch depth = 5 mm

(b) Notch depth = 10 mm

(c ) Notch depth = 15 mm

(d) Notch depth = 20 mm

Figure 6: Variation of predicted remaining life with crack depth for UHSC beam (250*50*50mm)

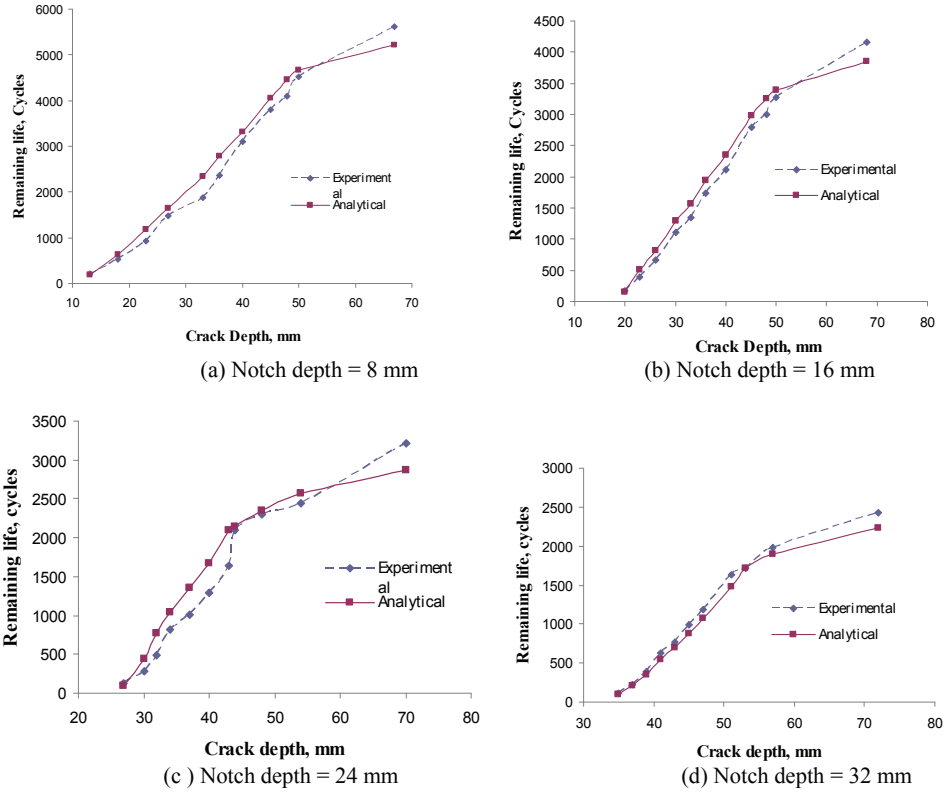


Figure 7: Variation of predicted remaining life with crack depth for UHSC beam (400*50*80mm)

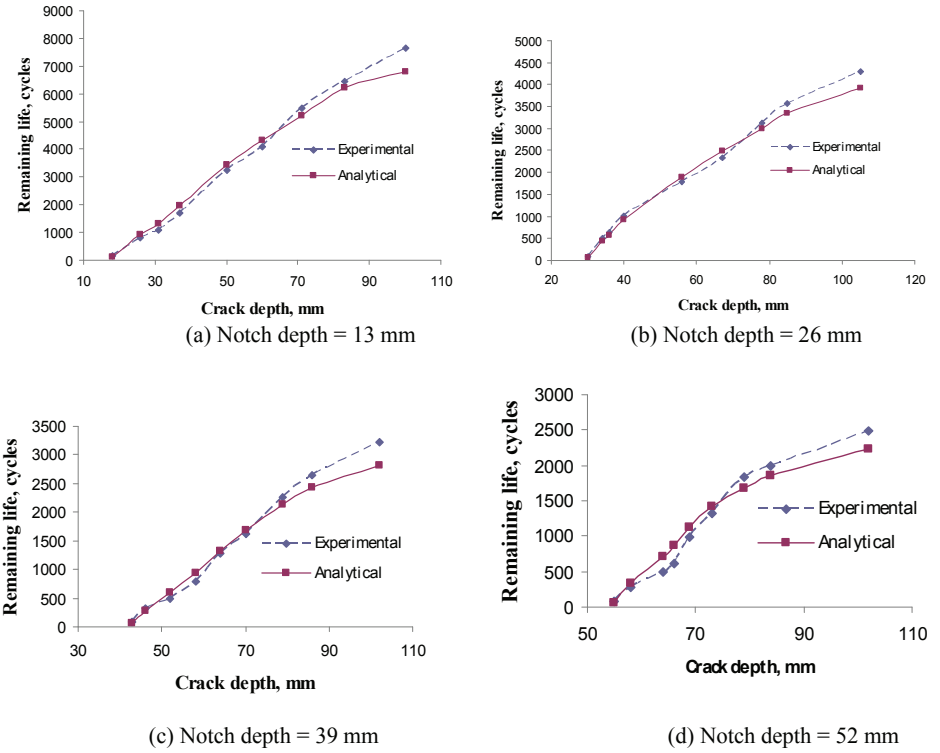


(a) Notch depth = 13 mm

(b) Notch depth = 26 mm

(c) Notch depth = 39 mm

(d) Notch depth = 52 mm

Figure 8: Variation of predicted remaining life with crack depth for UHSC beam (650*50*130mm, notch depth = 13, 26, 39, 52 mm)

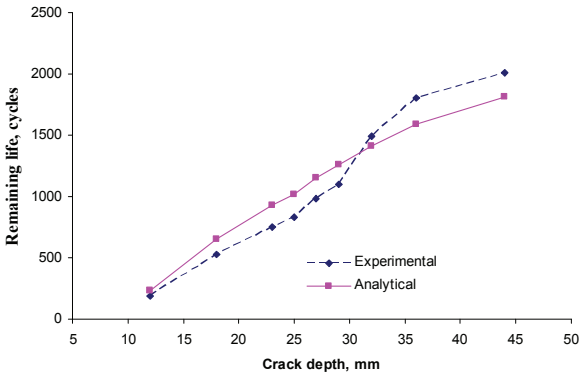


Figure 9: Variation of predicted remaining life with crack depth for HSC1 beam (500*50*100mm, notch depth = 20mm)

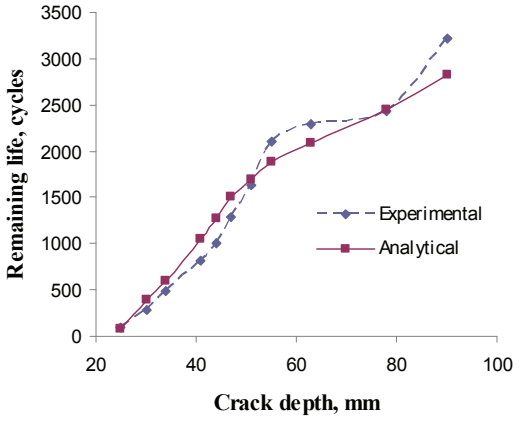


Figure 10: Variation of predicted remaining life with crack depth for HSC1 beam (250*50*50mm, notch depth = 5mm)

## 6 Summary and concluding remarks

Flexural fatigue tests have been conducted on HSC, HSC1 and UHSC specimens. Two specimens for each notch depth have been tested under load control. A stress ratio of 0.2 is maintained for all the specimens. At regular intervals, crack depth vs number of cycles has been recorded for HSC1 and UHSC specimens. It is observed from the studies that (i) the failure patterns of HSC1 and UHSC beams indicate ductility as the member was intact till the crack propagated up to 90% of the beam depth and (ii) the remaining life decreases with increases of notch depth. The failure of the specimen under fatigue loading is influenced by the frequency of loading. It is evident from the studies that the fibers are able to provide sufficient tensile reinforcement across the cracks and have sufficient fatigue resistance to stabilize the response of the specimen under these loading conditions. A "Net K" model has been proposed by using non-linear fracture mechanics principles for crack growth analysis and remaining life prediction. SIF (K) has been computed by using the principle of superposition. More importantly, the method of superposition employed in the net K model follows from the method adopted by Dugdale, Irwin while doing plasticity correction in metals. Infact, the material UHSC is closer to metals and such a method would be more appropriate. Various tension softening models such as linear, bi-linear, tri-linear, exponential and power curve have been presented with appropriate expressions. Bi-linear tension softening relationship obtained from the inverse analysis has been used to consider the cohesive the stresses acting ahead of the crack tip. Numerical studies have been

conducted on three point bending concrete structural component under constant amplitude loading. The predicted remaining life values have been compared with the corresponding experimental observations and it is noted that they are in good agreement with each other. This type of study will be useful for design of similar specimens/structural components subjected to fatigue loading.

**Acknowledgement:** We acknowledge with thanks the valuable technical suggestions and support provided by our colleagues, Dr. G.S. Palani, Mr S. Maheshwaran, Ms. Smitha Gopinath, Mr V. Ramesh Kumar, Scientists and Ms. B. Bhuvaneswari, Quick Hire Fellow, during the course of this investigation. The help and support provided by the staff of Advanced Materials Laboratory, CSIR-SERC to carry out the experiments is greatly acknowledged. This paper is being published with the permission of the Director,CSIR- SERC, Chennai, India.

## References

**Baluch, M.H.; Qureshy, A.B.; Azad, A.K. (1987):** Fatigue crack propagation in plain concrete. Proc., SEM/RILEM Int. conf. on fracture of concrete and rocks, p. 80-87.

**Bazant, Z.P. (1992):** Fracture mechanics of concrete Structures. Elsevier Applied Science, London.

**Bazant, Z.P.; Xu, K. (1991):** Size effect in fatigue fracture of concrete. *ACI mat. J* . vol. 88, pp.390-399.

**Bazant, Z.P.; Pfeiffer, P.A. (1987):** Determination of Fracture Energy Properties from Size Effect and Brittleness Number. *ACI Material Journal*, vol. 84, pp. 463-480.

**Bazant, Z.P.; Schell, W.F. (1993):** Fatigue fracture of high strength concrete and size effect. *ACI Mat. J.* vol.90, pp.472-478.

**Goltermann, P.; Johansen, V.; Palbol, L. (1997):** Packing of Aggregates: An Alternate Tool to Determine the Optimal Aggregate Mix. *ACI Material Journal*, pp.435-443.

**Ingraffea, A.R. (1977):** Discrete Fracture Propagation in Rock: Laboratory Tests and Finite Element Analysis. Ph.D. Dissertation, University of Colorado, Boulder.

**Kaplan, M.F. (1961):** Crack Propagation and the Fracture of Concrete. *ACI Journal,* vol.58, pp.591-610.

**Mingzhe, A.N.; Ziruo, Y.U.; Sun Meili.; Zheng Shuaiquan.; Liang Lei. (2010):** Fatigue Properties of RPC under Cyclic Loads of Single-stage and Multi-level Amplitude. *Journal of Wuhan University of Technology-Material Science Ed;* pp.167-

173.

**Peiwei, G.; Deng Min.; Naiqian, F. (2001):** Influence of Superplasticiser and Superfine Mineral Powder on the Flexibility, Strength and Durability of HPC. *Cement and Concrete Research*, vol.31, pp.703-706.

**Perdikaris, P.C.; Calomino, A.M. (1987):** Kinetics of crack growth in plain concrete. Proc., SEM/RILEM Int. conf. on fracture of concrete and rocks, p.64-69.

**Prasad, M.V.K.V.; Krishnamoorthy, C.S. (2002):** Computational model for discrete crack growth in plain and reinforced concrete. *Comput Method Appl Mech Engg,* vol. 191, pp.2699–2725.

**Richard, P.; Cheyrezy, M.H. (1994):** Reactive powder concretes with high ductility and 200–800 MPa compressive strength. *ACI SP144;* vol. 4, pp. 507–18.

**Richard, P.; Cheyrezy, M.H. (1995**): Composition of reactive powder concretes. *Cement & Concrete Research*, vol.25, no.7, pp.1501-1511.

**Shah, S.P.; Swartz, S.E. (1995):** Fracture Mechanics of Concrete: Applications of Fracture Mechanics to Concrete. Rock and other Quasi-brittle Material, John Wiley & Sons, Inc, New York.

**Slowik, V.; Beate Villmann, B.; Bretschneider, N.; Villmannm, T. (2006):** Computational aspects of inverse analyses for determining softening curves of concrete. *Comput Method Appl Mech Engg,* vol.195, pp.7223–7236.

**Subramaniam, V.K.; Neil, E.F.; Popovics, S.J.; Shah, S.P. (2000):** Crack propagation in flexural fatigue of concrete. *Jl Engg Mechanics*, vol.126, no.9, pp.891-898.

**Tada, H.; Paris, P.C.; Irwin, G.R. (1985):** The Stress Analysis of Cracks Handbook. $2^{nd}$ ed., Paris Productions, St. Louis. MO.

**Takashi Matsumoto, Victor C Li. (1999):** Fatigue life analysis of fiber reinforced concrete with a fracture mechanics based model. *Cement and Concrete Composites*, vol.21, pp. 249-261.

**Thomas C Gasser, Gerhard A Holzapfel. (2005):** Modeling 3D crack propagation in unreinforced concrete using PUFEM. *Comput Method Appl Mech Engg*, vol.194, pp.2859–2896.

**Toumi Bascos, A.; Turatsinze, A. (1998):** Crack propagation in concrete subjected to flexural cyclic loading. *Materials and Structures,* vol.31, pp. 451-458.

**Wu, Z.; Yang, S.; Hu, X.; Zheng, J. (2006):** An analytical model to predict the effective fracture toughness of concrete for three-point bending notched beams. *Engg. Fract. Mech*, vol.73, no.15, pp.2166-2191.